

X-ray radiation of the jets and the supercritical accretion disk in SS 433

Sergei Fabrika¹ and Alexei Medvedev²

¹Special Astrophysical Observatory,
 369167, Nizhij Arkhyz, Russia
 email: fabrika@sao.ru

²Moscow State University,
 119992, Moscow, Russia
 email: a.s.medvedev@gmail.com

Abstract. The observed X-ray luminosity of SS 433 is $\sim 10^{36}$ erg/s, it is known that all the radiation is formed in the famous SS 433 jets. The bolometric luminosity of SS 433 is $\sim 10^{40}$ erg/s, and originally the luminosity must be realized in X-rays. The original radiation is probably thermalized in the supercritical accretion disk wind, however the missing more than four orders of magnitude is surprising. We have analysed the XMM-Newton spectra of SS 433 using a model of adiabatically and radiatively cooling X-ray jets. The multi-temperature thermal jet model reproduces very well the strongest observed emission lines, but it can not reproduce the continuum radiation and some spectral features. We have found a notable contribution of ionized reflection to the spectrum in the energy range from ~ 3 to 12 keV. The reflected spectrum is an evidence of the supercritical disk funnel, where the illuminating radiation comes from deeper funnel regions, to be further reflected in the outer visible funnel walls ($r \geq 2 \cdot 10^{11}$ cm). The illuminating spectrum is similar to that observed in ULXs, its luminosity has to be no less than $\sim 10^{39}$ erg/s. A soft excess has been detected, that does not depend on the thermal jet model details. It may be represented as a BB with a temperature of $T_{bb} \approx 0.1$ keV and luminosity of $L_{bb} \sim 3 \cdot 10^{37}$ erg/s. The soft spectral component has about the same parameters as those found in ULXs.

Keywords. X-rays: individual (SS 433), accretion, accretion disks, black hole physics

SS 433 is the only known persistent superaccretor in the Galaxy – a source of relativistic jets (Fabrika (2004) for review). This is a massive close binary, where the compact star is most probably a black hole. Its intrinsic luminosity is estimated to be $\sim 10^{40}$ erg/s, with its maximum located in non-observed UV region. Almost all the observed radiation is formed in the supercritical accretion disk, and the donor star contributes less than 20 % of the optical radiation. The extreme luminosity of the object is supported by a very well measured kinetic luminosity of the jets, $\sim 10^{39}$ erg/s, both in direct X-ray and optical studies of the jets and in the studies of the jet-powered nebula W 50. At the same time we know that practically all the energy at the accretion onto a relativistic star is released in X-rays. This means that the observed radiation of SS 433 is a result of thermalization of the original radiation in the strong wind forming in the supercritical disk.

The observed X-ray luminosity of SS 433 is $\sim 10^{36}$ erg/s and it is believed that all the X-rays come from the cooling X-ray jets (Kotani *et al.* 1996; Marshall, Canizares, & Schulz 2002; Brinkmann, Kotani, & Kawai 2005). The observed X-ray radiation is at least four orders of magnitude less than the bolometric luminosity, which originally must be released in X-rays. Both the orientation of SS 433 and the visibility conditions do not allow us to see any deep areas of the supercritical accretion disk funnel. However, the strong mass loss of the accretion disk gives us a hope for detecting some indications of

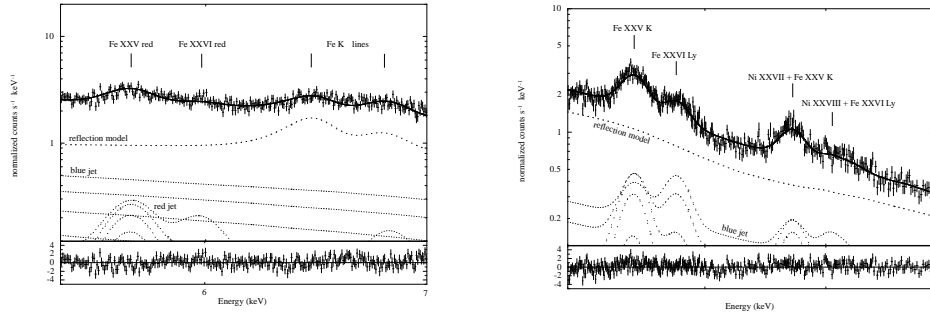


Figure 1. Observed spectrum of SS 433 (orbit 707, $\psi \sim 0$) with the thermal jet model components and the additional reflection model in two spectral regions 5.0–7.0 (left) and 7.0–10.0 keV (right). The total model spectrum is shown with solid line. The reflection model explains well the fluorescence iron line at 6.4 keV, the recombination iron $K\alpha$ line of Fe XXV at 6.7 keV and the iron absorption edge (Kubota *et al.* 2007) at ~ 8 –9 keV.

the funnel radiation. The goal of our study is to find these indications of the funnel in the SS 433 X-ray radiation.

We have analysed XMM spectra of SS 433 with a well-known standard model of the adiabatically cooling X-ray jets, taking into account cooling by radiation (Medvedev & Fabrika 2010). We have selected only those observations (Brinkmann, Kotani, & Kawai 2005) with highest S/N, where disk was not eclipsed by the donor and was the most open to the observer (precessional phases $\psi = 0.04$ and 0.84). We confirm that the jet model reproduces the iron emission line fluxes quite well. However, the thermal jet model alone can not reproduce the continuum radiation in the XMM spectral range. We use then the multi-temperature thermal jet model together with the REFLION ionized reflection model (Ross & Fabian 2005). We divide the whole spectrum into four parts (0.8–2.0, 2.0–4.0, 4.0–7.0 and 7.0–12.0 keV) and find the reflection model parameters independently in each part, but with the same jet parameters and the same IS absorption N_H .

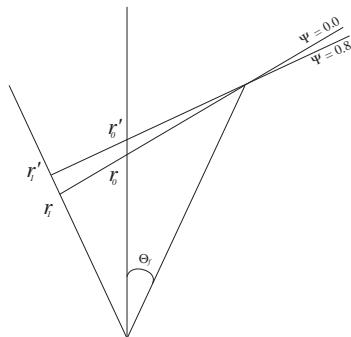


Figure 2. A sketch of the funnel and the blue jet visibility at two precessional phases considered. r_0 (r_0') is the distance between the base of the visible jet and the top of the cone (the bottom of the funnel). r_1 (r_1') is the distance between the base of the visible funnel wall and the top of the cone.

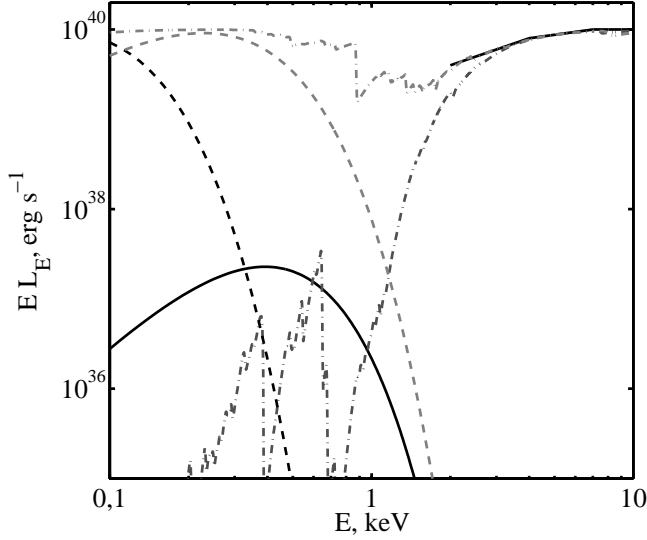


Figure 3. Additional components in X-ray spectrum of SS 433 (the thermal jet component is not shown). The illuminating incident radiation found in reflection model is shown by solid lines (arbitrary scaled to $EL_E = 10^{40}$ erg/s) in three energy ranges: 2.0–4.0 keV ($\Gamma = 1.0$), 4.0–7.0 keV ($\Gamma = 1.6$) and 7.0–12.0 keV ($\Gamma = 2.0$). The soft BB component ($T_{bb} = 0.1$ keV, $L_x \sim 3 \cdot 10^{37}$ erg/s) detected in the 0.8–2.0 keV energy range is shown by solid line. There are two originally the same flat spectra after absorption in ABSORI model with $N_H = 10.0 \times 10^{22} \text{ cm}^{-2}$, $\xi = 150$ (grey dash-dotted line) and $N_H = 6.0 \times 10^{22} \text{ cm}^{-2}$, $\xi = 3$ (bold dash-dotted line). There are two MCF (multi-colour funnel model) non-absorbed spectra with $r_1 = 1.7 \cdot 10^{11} \text{ cm}$ (bold dotted line) and $r_1 = 5 \cdot 10^{10} \text{ cm}$ (grey dotted line).

Fig. 1 shows two spectral regions with the "thermal jet + reflection" model, we find quite a good representation of the spectra. The reflection model explains well the spectral features unexplained before. We find that the ionization parameter is about the same in the different X-ray ranges, $\xi \sim 300$, which indicates a highly ionized reflection surface. The illuminating radiation photon index changes from flat, $\Gamma \approx 2$, in the 7–12 keV range to $\Gamma \approx 1.6$ in the range 4–7 keV and to $\Gamma \leq 1$ in the range 2–4 keV.

Fig. 2 shows the jet and the probable funnel wall visibility at the two precessional phases studied. We found the visible blue jet base is $r_0 \approx 2 \cdot 10^{11} \text{ cm}$, the gas temperature at r_0 is $T_0 \approx 17 \text{ keV}$. The IS gas column density is $N_H \sim 1.5 \cdot 10^{22} \text{ cm}^{-2}$, which is in good agreement with the IS extinction found in optical and UV observations. We confirm the previous finding (Kotani *et al.* 1996; Brinkmann, Kotani, & Kawai 2005) that the red jet is probably not seen (blocked) in the soft energy range of 0.8–2.0 keV. However, both the model with blocked the red jet portions, and the model with the whole red jet visible (but with some higher N_H) give the same result, that the thermal jet model alone can not explain the soft continuum. We also confirm that Nickel is highly overabundant, at least 10 times, in the jets (Kotani *et al.* 1996; Brinkmann, Kotani, & Kawai 2005).

We have not found any evidences of the reflection in the soft 0.8–2.0 keV energy range, instead the soft excess is detected in spectra. The soft excess does not depend on the thermal jet model details, this model alone can not explain the soft continuum. We suppose that in the soft X-rays we observe direct radiation of the visible funnel wall. We represented this component (Fig. 3) as a black body radiation with a temperature of

$T_{bb} \approx 0.1$ keV and a total luminosity (being observed face-on at $r > r_1 = 1.7 \cdot 10^{11}$ cm) of $L_{BB} \sim 3 \cdot 10^{37}$ erg/s. The soft excess may be also fitted with a multicolour funnel (MCF) model (Fabrika *et al.* 2006). The soft excess is observed in the spectra of ULXs with the soft component temperature of $T \sim 0.1$ keV (Stobart, Roberts, & Wilms 2006), which is similar to that found in SS 433. If the ULXs or some of them are nearly face-on versions of SS 433, one may adjust their soft X-ray components to the outer funnel walls radiation (Poutanen *et al.* 2007).

We conclude that the additional reflected spectrum is an indication of the funnel radiation. The illuminating radiation spectrum is flat in the range of 7–12 keV, as it is expected in supercritical accretion disks (Poutanen *et al.* 2007). Comptonization may extend and flatten the spectrum to higher energies. With multiple scatterings in the funnel the hard radiation may survive absorption. The observed reflected luminosity in this 7–12 keV spectral range is $L_{refl} \sim 10^{36}$ erg/s. We find that the illuminating luminosity has to be no less than $\sim 10^{39}$ erg/s (Medvedev & Fabrika 2010).

In the range 2.0–7.0 keV the additional reflected spectrum is curved (Fig. 3). Therefore we expect an existence of an absorbing (reflecting) medium inside the funnel, which produces such a curved spectrum of radiation, illuminating the outer reflected surface. Presumably this medium is the deep funnel regions. The recent data show (Stobart, Roberts, & Wilms 2006; Berghea *et al.* 2008) that ULXs possess curvature and rather flat X-ray spectra, which are difficult to interpret with a single-component or any other simple model. We note that the main properties of the ULXs X-ray spectra are similar to those restored additional spectral components in SS 433, the ULXs may be "face-on" versions of SS 433.

The softer (2–7 keV) part of the illuminating spectrum (Fig. 3) carries a trace of absorption. This is assumed to be due to the multiple scatterings in the funnel. It is important to note that an existence of He- and H-like absorption edges at about zero velocity is a mandatory property of the funnel spectrum to be able to produce the observed jet velocity due to the line-locking mechanism. The jet velocity value, $v_j \approx 0.26c$, and its unique stability, where the velocity does not depend on the activity state, indicate that the jet acceleration must be controlled by the line-locking mechanism (Shapiro, Milgrom, & Rees 1986; Fabrika 2004).

References

- Berghea C. T., Weaver K. A., Colbert E. J. M., Roberts T. P., 2008, *ApJ*, 687, 471
 Brinkmann W., Kotani T., Kawai N., 2005, *A&A*, 431, 575
 Fabrika S., 2004, *ASPRv*, 12, 1
 Fabrika S., Karpov S., Abolmasov P., Sholukhova O., 2006, *IAUS*, 230, 278
 Kotani T., Kawai N., Matsuoka M., Brinkmann W., 1996, *PASJ*, 48, 619
 Kubota K., Kawai N., Kotani T., Ueda Y., & Brinkmann W., 2007, *ASPC*, 362, 121
 Marshall H. L., Canizares C. R., Schulz N. S., 2002, *ApJ*, 564, 941
 Medvedev A., Fabrika S., 2010, *MNRAS*, 402, 479
 Poutanen J., Lipunova G., Fabrika S., Butkevich A. G., Abolmasov P., 2007, *MNRAS*, 377, 1187
 Ross R. R., Fabian A. C., 2005, *MNRAS*, 358, 211
 Shapiro P. R., Milgrom M., Rees M. J., 1986, *ApJS*, 60, 393
 Stobart A.-M., Roberts T. P., Wilms J., 2006, *MNRAS*, 368, 397

